Available online at www.sciencedirect.com
ScienceDirect
Journal of Hazardous Materials 156 (2008) 327–334
Journal of Hazardous Materials
www.elsevier.com/locate/jhazmat

Confinement of fire-induced smoke and carbon monoxide transportation by air curtain in channels

L.H. Hu *, J.W. Zhou, R. Huo, W. Peng, H.B. Wang

State Key Laboratory of Fire Science, University of Science and Technology of China, Hefei, Anhui, China

Received 19 August 2007; received in revised form 10 December 2007; accepted 10 December 2007
Available online 23 December 2007

Abstract

Experimental and numerical studies were performed in this paper to study the possibility of utilizing air curtain for confinement of fire-induced smoke and carbon monoxide transportation along channels. Bench scale experiments were preliminarily performed in a 3.6 m long model channel. Complementary computational fluid dynamics (CFD) simulation was carried out by Fire Dynamics Simulator (FDS) for an 88 m long full scale channel, in order to see the longitudinal carbon monoxide concentration distribution along the real channel with air curtain discharged. Results showed that both the smoke and CO gases released by the fire were well confined to almost remain in the near fire region of the channel at one side of the air curtain. The gas temperature and CO concentration in the protection zone at the other side reduced significantly by an exponential trend with the increase of discharge velocity of the air curtain. These indicated that the air curtain can be an effective measure for confining the transportation of smoke and carbon monoxide species in long channel fires.

Keywords: Channel fire; Air curtain; Confinement; Smoke; Carbon monoxide

1. Introduction

Statistics have shown [1] that smoke and toxic gases, such as carbon monoxide, are the most fatal factor in fires, and about 85% of people killed in building fires were killed by toxic smoke. The smoke particle lowers down the visibility range in the space resulting in that the people cannot find the way to escape out. And the toxic gases directly harm and kill the evacuee. Taking appropriate methods to confine the spread of the smoke and toxic gases in case of a fire is a serious concern for smoke management in buildings. Fire in a long channel, such as a tunnel, is a special topic in building fire research, due to its different aspect ratio from normal room enclosures. Channels, such as aisles or corridors, are also ordinary seen in hotels, underground shopping streets or some other large space buildings, where the personal load is very large at the same time. Once these buildings are on fire, the channel is one of the main approaches for smoke spread. And at the same time, these channels also usually constitute parts of the evacuation route in the building during fire emergency. So enough attention should be paid to prevent smoke or toxic gases, such as carbon monoxide, released by the fire from spreading along the channels [2].

Solid obstructions, such as walls, boards, doors, light smoke screens, etc., are traditionally used for smoke compartmentation in buildings. But sometimes these measures are not available or practical in these channels due to limitation of the clear height available or their special function. The solid obstructions standing there hamper the evacuation at the early stage of the fire even when the smoke has not spread to their positions. A more appropriate measure, which does not influence the normal usage of the channel with less occupying space needed, nor hampers the people from evacuation, should be adopted. So, a method of using air curtain for confinement of smoke and carbon monoxide transportation in a channel fire is discussed in this paper. The primary intention is to confine the smoke and toxic gases released by the fire to remain in the near fire region. So, the pollution to the indoor air environment of other spaces can be reduced and limited.

Air curtains have been widely used in building entrance or shop windows, for keeping cool air at one side and the hot air at the other side [3–6], reducing chemical species transfer [7], or flow regulation in mine airway [8] and other applications

* Corresponding author. Tel.: +86 551 3606446; fax: +86 551 3601669.
E-mail address: hlh@ustc.edu.cn (L.H. Hu).

0304-3894/$ – see front matter © 2008 Published by Elsevier B.V.
doi:10.1016/j.jhazmat.2007.12.041

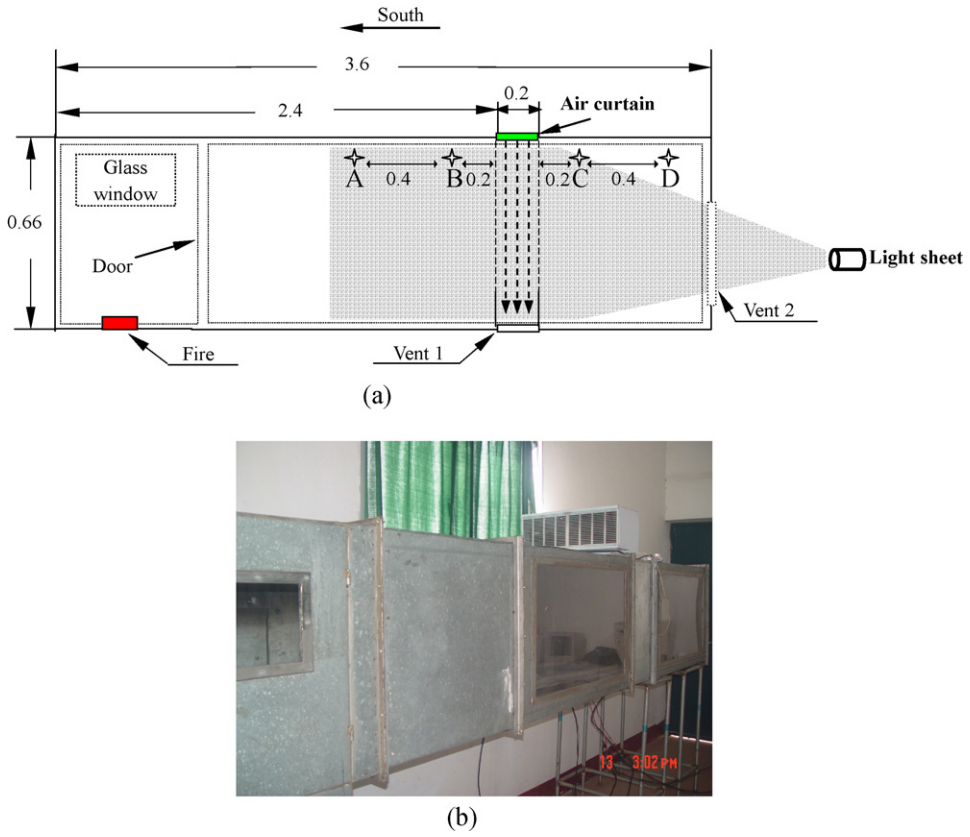

Fig. 1. Design of experimental apparatus: (a) schematic view (unit: m) and (b) photo of experimental rig.

[9–14]. Guyonnaud and Solliec [5] studied the usage of air curtain to reduce the heat and mass transfer from one zone to another subjected to different environmental or climatic condition. Utilization of air curtain in tunnels was also preliminary discussed and reported [12–14]. The latest work reported on air curtain application was performed by Gupta et al. [12]. But they only considered the confinement of ethane gas dispersion without buoyancy effect. However, fundamental study on the confinement of fire-induced buoyancy-driven smoke flow, especially transportation of toxic carbon monoxide, by air curtain is still very scarce.

Experimental and numerical studies were performed in this paper to study the possibility of using air curtain for confinement of smoke and carbon monoxide transportation in channel fires. A series of bench scale experiments were performed in a 3.6 m long model channel. A light sheet was used for visualization

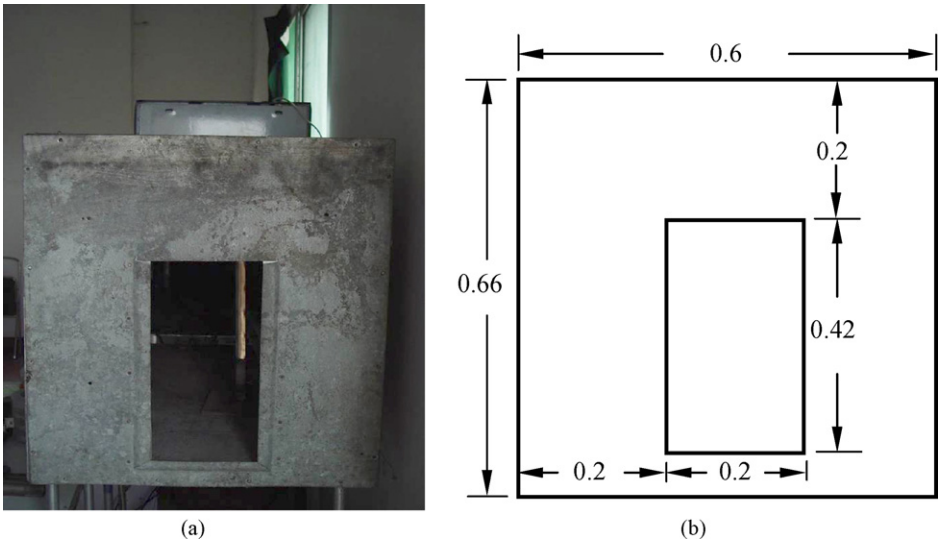

Fig. 2. Opening at the north end of the model channel: (a) photo and (b) dimensions (unit: m).

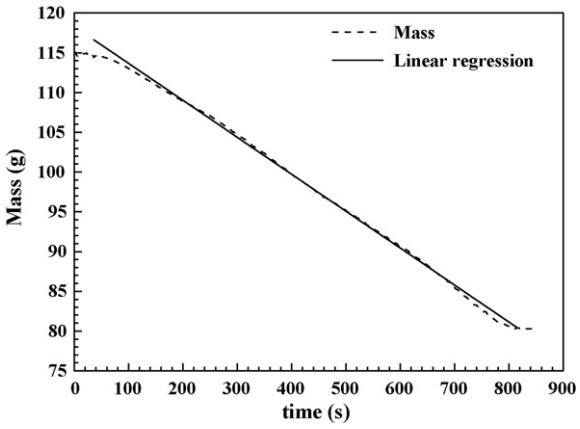

Fig. 3. Mass loss rate of the pool fire.

of the results of smoke confinement by the air curtain. The gas temperature and CO concentration in the protected zone with the air curtain discharged were compared with that with air curtain non-discharged. Complementary computational fluid dynamics (CFD) simulations were carried out by Fire Dynamics Simulator (FDS) in an 88 m long full scale channel, in order to see the field distribution of carbon monoxide and the longitudinal carbon monoxide concentration deduction along the channel with air curtain discharged.

2. Experimental model

Preliminary bench scale experiments were conducted in a 3.6 m long model channel as shown in Fig. 1. The cross-section of the channel is 0.6 m (width) × 0.66 m (height). As shown in Fig. 1(b), the model channel consists of four sections. The first section is designed as combustion region with a window and a door. All these sections are made of steel board except the front faces of Sections 3 and 4, which are made of toughened glass for visualization. The lining material of the inner surface is plasterboard. The southern end of the channel, the door and the window of the combustion section is closed. There is an opening of 0.2 m (width) × 0.42 m (height) in the north end as shown in Fig. 2. A light sheet is launched to go through the north opening into the channel, as shown in Fig. 1, for visualization of the effect of smoke confinement.

Fig. 4. Visualization of smoke confinement by the light sheet.

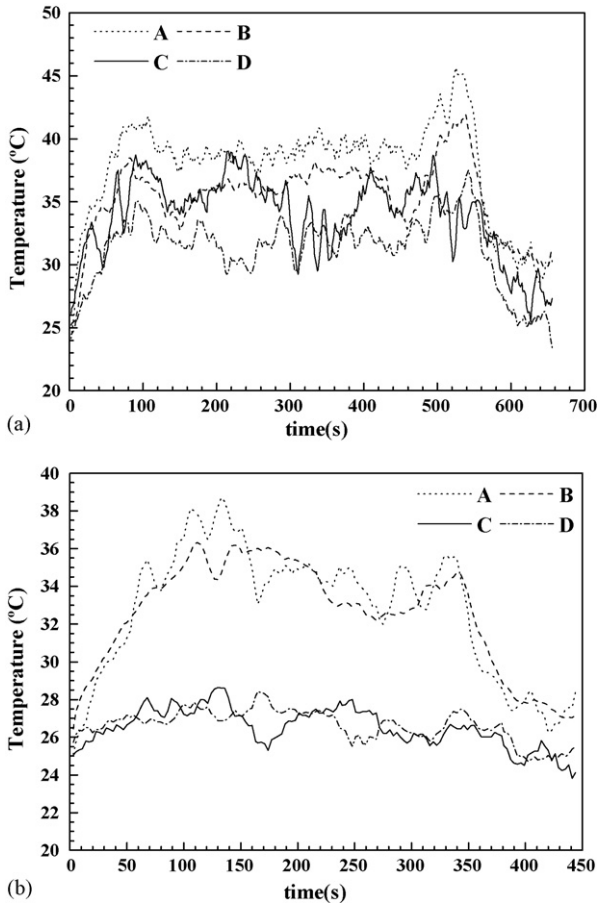

Fig. 5. Smoke temperatures at two sides of the air curtain: (a) with air curtain non-discharged and (b) with air curtain discharged (for v=3 m/s).

A circular pool fire with diameter of 0.086 m was burned as fire source. Diesel oil was used as the fuel. An electronic balance with weight resolution of 0.1 g was used to measure the transient mass of the burning diesel pool. The data acquisition interval for the mass was 1 s. The steady burning mass loss rate of the pool fire was deduced from mass loss history measured by the balance, as shown in Fig. 3. The heat release rate (HRR) of

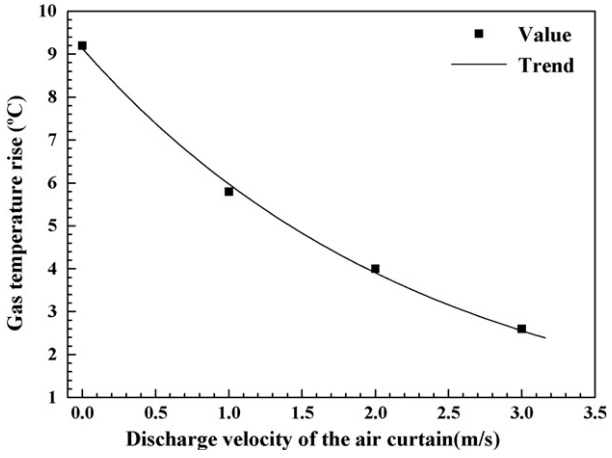

Fig. 6. Temperature deduction for the protected zone by air curtain with different outlet discharging velocities.

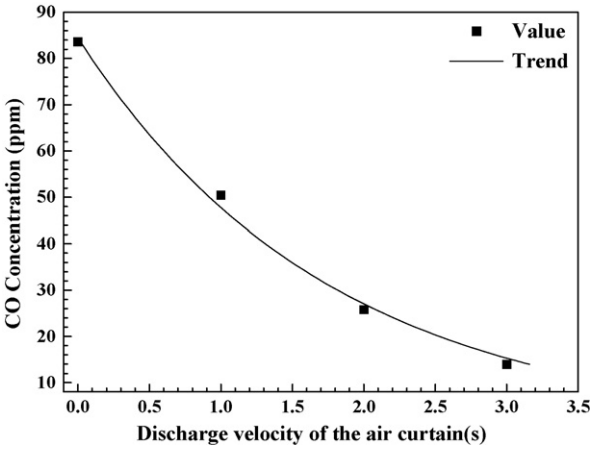

Fig. 7. CO concentration deduction for the protected zone by air curtain with different outlet discharging velocities.

the pool fire was further deduced from the burning mass loss rate with combustion efficiency assumed to be 1 for such a small pool fire. The HRR of the pool fire was then deduced to be about 2 kW, taking the heat of combustion of diesel oil to be 42,000 kJ/kg.

An air curtain device was installed between the top of Sections 3 and 4, being 2.4 m away from the southern end. The horizontal width of the air curtain was 0.2 m. There was also an opening with width of 0.2 m at the floor level of the channel, directly facing the outlet discharging vent of the air curtain device. The air blowing out from the air curtain device flowed down out of the experimental model channel from this floor opening, thus to form an air curtain. The rotating speed of the air curtain device, thus the outlet discharging velocity, was controlled by the input voltage. During the tests, three levels of outlet discharging velocities were considered: 1, 2 and 3 m/s, by controlling the input voltage to be of 65, 80 and 90 V, respectively.

Smoke temperatures below the ceiling along the channel were measured at four positions: A–D as shown in Fig. 1. These positions were all 0.12 m below the channel ceiling. A combustion product analyzer was used for measuring the CO concentration in the protected zone of the channel. Its probe was located at position C.

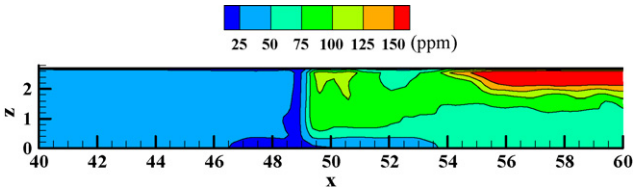

Fig. 9. Field distribution of CO concentration simulated by FDS at the two sides of the air curtain in the channel.

3. Experimental results

Total four tests were carried out with air curtain discharging velocities of 1, 2 and 3 m/s and the air curtain closed. A typical photo of smoke confinement by the air curtain in this channel as visualized by the light sheet is shown in Fig. 4. A clear interface was shown between the smoke zone and the protected zone, at the vertical plane where the air curtain discharged. It seemed that the smoke was well confined to almost remain in the near fire region at the southern side of the air curtain. The protected zone at the north side of the air curtain was shown to be nearly free of smoke with high visibility.

The smoke temperatures measured at positions A–D with air curtain discharged and non-discharged are typically shown in Fig. 5. It was shown in Fig. 5(a) that with the air curtain non-discharged, the temperature seemed to decrease continuously longitudinally from position A to position D. However, as shown in Fig. 5(b) with the air curtain discharged, the four temperature curves were obviously divided into two groups: the curves of A and B with much higher temperatures in the smoke zone, and those of C and D with much lower temperatures in the protected zone. This also indicated that the hot buoyant smoke flow was mainly confined to remain in the near fire region by the air curtain.

Fig. 6 presents the smoke temperatures rise above the ambient condition measured at position C under different air curtain discharging velocities. It was shown that the smoke temperature rise in the protected zone decreased fast with the increase of the discharge velocity. The CO concentration measured at position C is plotted against the discharging velocity of the air curtain in Fig. 7. The CO concentration in the protected zone also decreased fast with the increase of the discharging velocity. However, as both can be seen in Figs. 5 and 6, the decay of temperature rise and CO concentration in the pro-

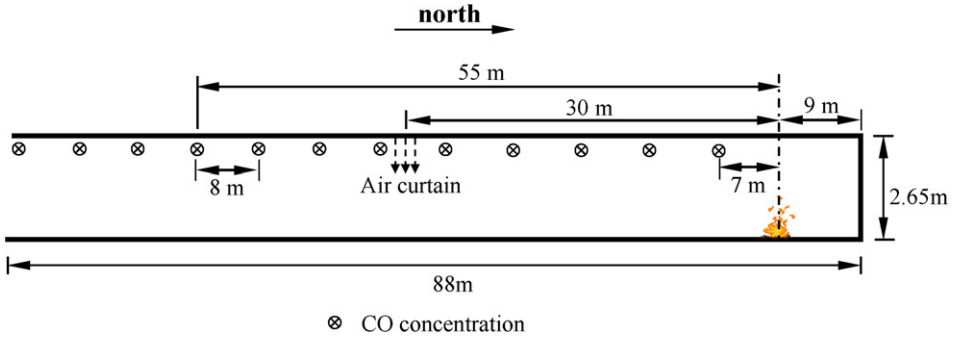

Fig. 8. Utilization of air curtain in a full scale 88 m long channel.

tected zone with the increase of the discharging velocity of the air curtain can be both well correlated by an exponential regression, with correlation coefficient both of 0.99. It can be preliminarily seen from all above that the air curtain can play a good role in decreasing the smoke particle concentration to provide much better visibility, as well as lowering down the gas temperature and the CO concentration of the protected zone.

4. CFD simulations

4.1. model configuration

Complementary computational fluid dynamics (CFD) simulation was further performed to see the confinement of fire-induced CO transportation by air curtain in a real scale channel. CFD simulations were carried out with fire dynamics simulator (FDS), a software package released by the National Institute of Standards and Technology (NIST), USA. It is now a popular CFD tool in fire related researches. A description of the software, many validation examples [e.g. 15,16], and a bibliography of related papers and reports may be found on the website [17]. The set of the Navier–Stokes equations for fire-driven fluid flow is solved numerically with large eddy simulation (LES). It is second-order accurate in space and time differences. The recent version of FDS 4.07 released in March, 2006 was used. A refined filtered dynamics sub-grid model is applied in the FDS model to account for the sub-grid scale motion of viscosity, thermal conductivity and material diffusivity [16,17]. The dynamic viscosity defined in FDS is

$$\mu_{ijk} = \rho_{ijk}(C_S\Delta)^2\,|S|$$

where C_S is an empirical Smagorinsky constant, Δ is $\delta x\delta y\delta z^{1/3}$ and $|S| = 2\left(\frac{\partial u}{\partial x}\right)^2 + 2\left(\frac{\partial v}{\partial y}\right)^2 + 2\left(\frac{\partial w}{\partial z}\right)^2 + \left(\frac{\partial u}{\partial x} + \frac{\partial v}{\partial y}\right)^2 + \left(\frac{\partial u}{\partial z} + \frac{\partial w}{\partial x}\right)^2 + \left(\frac{\partial v}{\partial z} + \frac{\partial w}{\partial y}\right)^2 - \frac{2}{3}(\nabla\cdot\vec{u})^2$

The term $|S|$ consists of second-order spatial differences averaged at the grid centre. The thermal conductivity k_{ijk} and material diffusivity D_{ijk} of the fluid are related to the viscosity μ_{ijk} in terms of the Prandtl number Pr and Schmidt number Sc by

$$k_{ijk} = \frac{c_p\mu_{ijk}}{Pr}, \qquad (\rho D)_{ijk} = \frac{\mu_{ijk}}{Sc}$$

Both Pr and Sc are assumed to be constant. The specific heat c_p is taken to be that of the dominant species of the mixture [16,17]. FDS had been formerly successfully applied to study the dispersion of propane under a leakage condition in a room [18] and contamination levels in near and far field in a warehouse facility under forced ventilation [19].

A full scale channel, as shown in Fig. 8, with length of 88 m, width of 8 m and height of 2.65 m was considered for CFD simulation. Full scale fire tests had formerly been conducted [20–22] in this long channel. Two pool fires with heat release rates (HRR) of 0.75 and 1.6 MW were burned with CO concentration measured at 55 m away from the fire and 2.2 m above the floor. The north end was closed with the south end half-opened for the channel. The ambient temperature was about 27.5 and 28 °C for the two tests, respectively. The internal boundary material of the simulated channel was set to be same as that in the experiments. The ceiling was set to be gypsum. The side wall and the floor were set to be concrete. Multi-mesh technology in FDS was applied. The near fire plume domain was with small grid size, 0.1 m(x) × 0.1 m(y) × 0.1 m(z) for one control volume, as complex combustion and physical process would

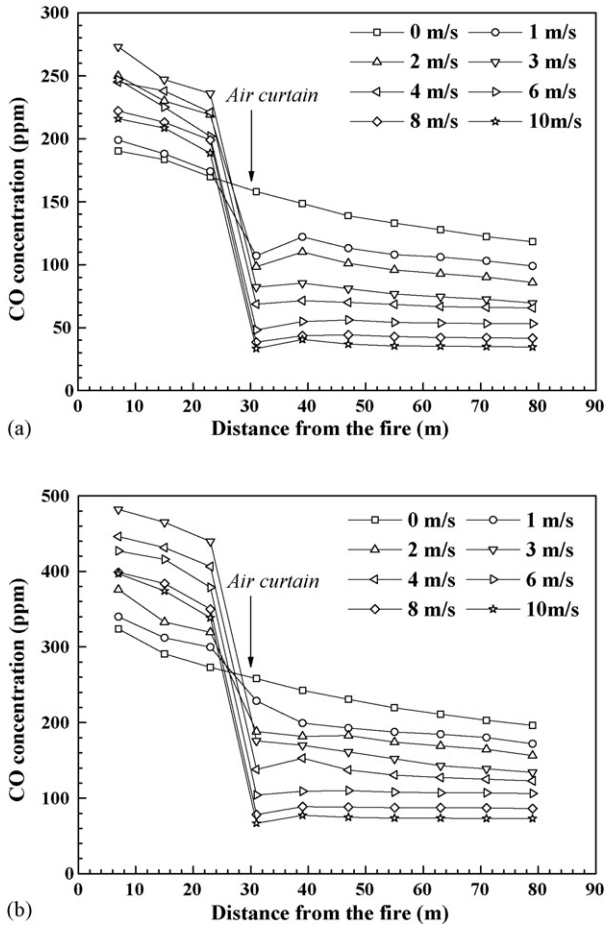

Fig. 10. Longitudinal CO concentration distribution along the channel: (a) 0.75 MW and (b) 1.6 MW.

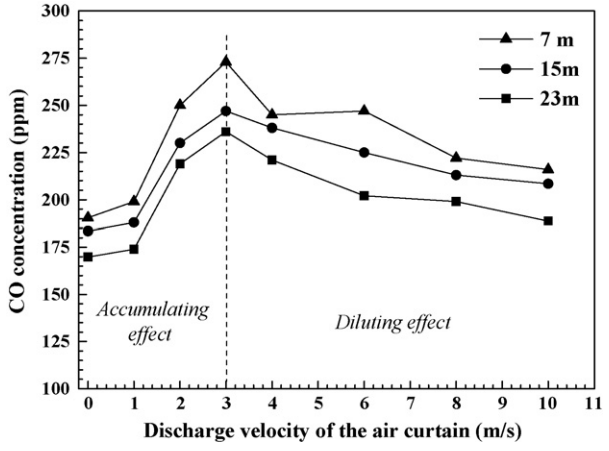

Fig. 11. Variation of CO concentration in the near fire confinement zone with discharging velocity of the air curtain.

occur in this domain. Other space was with a bit coarser grid sizes, 0.25 m(x) × 0.25 m(y) × 0.15 m(z) for one control volume. More detailed description on the channel and the full scale tests can be seen in the former report [22]. Validation of CO concentration prediction for fire in this channel had also been formerly reported [22] with good agreement between the predicted value and the measured value in the full scale tests. The same FDS model as that formerly validated [22] was used in the simulations of this paper. These included the same setting up of the grid system, the boundary condition, the HRR history of the fire, the combustion model and so on. Detailed information of these settings can be seen in the former report [22] and will not be described again here.

An air curtain with horizontal width of 0.2 m was set up at the ceiling of the channel, being 30 m away from the fire. It was set by the "VENT" command in FDS, which blowing fresh air vertically down into the channel. The outlet discharging velocities of the air curtain considered for the simulative cases were 1, 2, 3, 4, 6, 8 and 10 m/s. Under these different air curtain discharge discharging velocities, the longitudinal CO concentration distribution along the channel was computed at 10 positions, from 7 to 79 m away from the fire with same interval of 8 m and height of 2.45 m above the floor, to see the variation of CO concentration at the two sides of the air curtain.

4.2. Simulation results

The Field distribution of CO concentration simulated by FDS at the two sides of the air curtain in the channel is typically shown in Fig. 9. Fig. 10 presents the longitudinal CO concentration distribution along the channel with air curtain non-discharged and discharged under different out let velocities. It can be seen that the CO concentration dropped significantly at the position where the air curtained discharged. With air curtain discharged, the CO concentration in the near fire confined zone increased, while that in the protected zone at the other side decreased significantly. With the increase of the outlet discharging velocity, the CO concentration in the protected zone decreased. When the outlet discharging velocity was in the range of 1–3 m/s, the CO concentration in the protection zone seemed to still decrease slowly with the distance away from the fire. However, when it increased up to 4 m/s or more, the CO concentration seemed to vary little along the channel in the protected zone.

The variation of CO concentration in the near fire confined zone with the increase of the discharging velocity of the air curtain is shown in Fig. 11. The influence of air curtain discharge velocity on the CO concentration in the near fire confined zone was shown to fall into two different mechanisms. It was shown to be an accumulating effect when the discharging velocity of

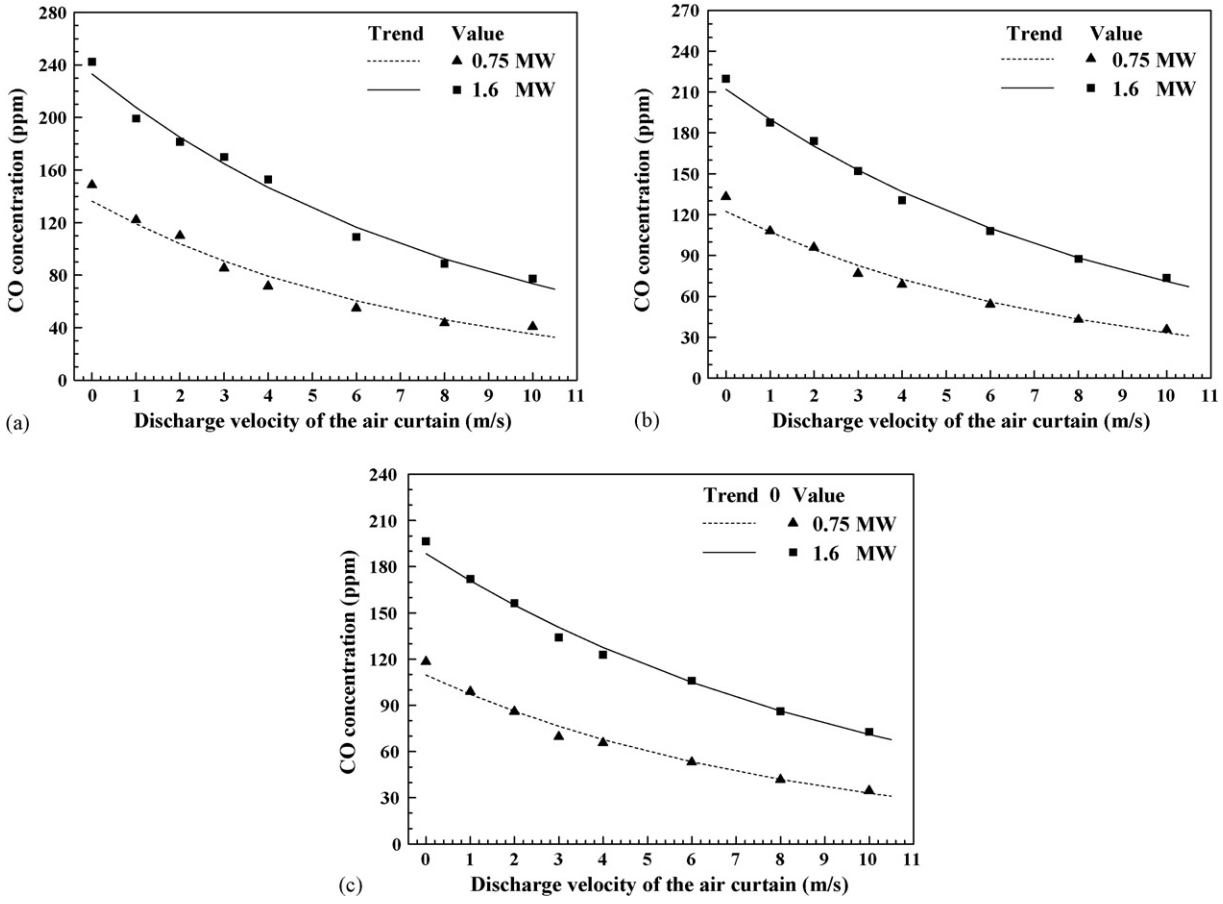

Fig. 12. Variation of CO concentration in the protected zone with discharging velocity of the air curtain: (a) 39 m away from the fire, (b) 55 m away from the fire and (c) 79 m away from the fire.

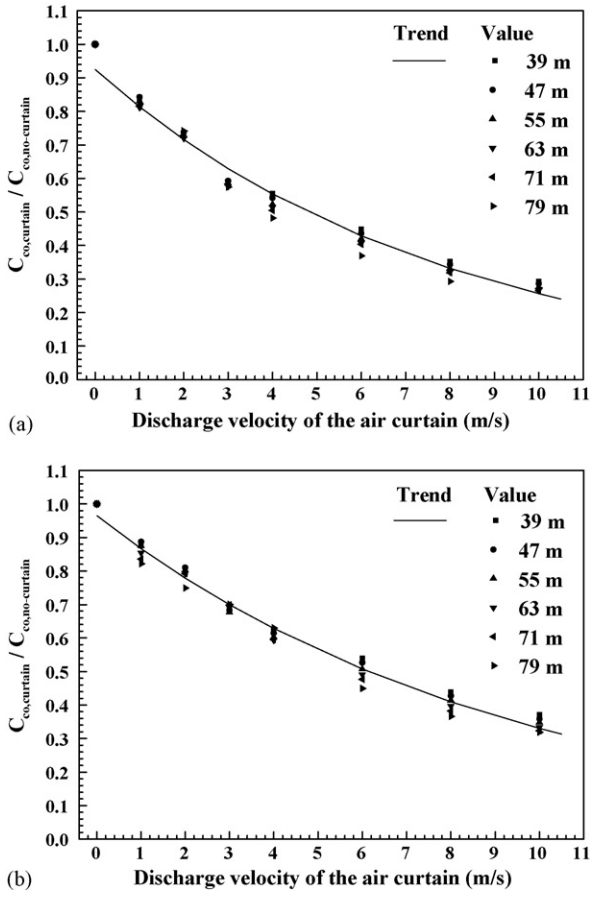

Fig. 13. Relative residual CO concentration under different air curtain discharging velocities: (a) 0.75 MW and (b) 1.6 MW.

air curtain was no more than 3 m/s, while to be a diluting effect for that up to 4 m/s and more. The CO concentration in the near fire confined zone increase with the increase of the discharging velocity of the air curtain when the discharging velocity was no more than 3 m/s. However, when the discharging velocity was up to 4 m/s or more, it decreased with the increase of the discharging velocity of the air curtain. The CO concentration in the near fire confined zone seemed to accumulate to a maximum level when the discharging velocity of the air curtain was at 3 m/s.

Fig. 12 presents the variation of CO concentration in the protected zone with the increase of the air curtain discharging velocity. Values at three typical positions: 39, 55 and 79 m away from the fire, are shown here. The CO concentration level in the protected zone reduced fast with the increase of the air curtain discharging velocity. Their relationship can be well correlated by exponential regression with correlation coefficient to be 0.96 (0.75 MW) and 0.99 (1.6 MW) for 39 m, 0.96 (0.75 MW) and 0.99 (1.6 MW) for 55 m, 0.99 (0.75 MW) and 0.99 (1.6 MW) for 79 m. The decay trends were same with that gotten in the bench scale model experiments. The relative residual CO concentration ($C_{co,\ curtain}/C_{co,\ no\text{-}curtain}$) levels simulated for different sampling positions in the protected zone are all plotted together against the air curtain discharging velocities in Fig. 13. All these values showed to be with the same trend and can be well approached by an exponential fitting.

5. Conclusions

Bench scale experiments and CFD simulations were carried out to study the possibility of using air curtain for smoke and CO confinement in channel fires. Results showed that the smoke and CO gas released by the fire were mainly confined to remain in the near fire region at one side of the air curtain, with gas temperature and CO concentration dropped significantly in the protected zone at the other side. The influence of the air curtain on the CO concentration in the near fire confinement zone was shown to be an accumulating effect when the discharging velocity was no more than 3 m/s, while to be a diluting effect for that up to 4 m/s and more. That is, the variation of CO concentration in the near fire confined zone firstly increase and then decreased with the increase of the air curtain discharging velocity. The CO concentration in the near fire confinement zone reached a maximum level at discharging velocity of about 3 m/s. However, the gas temperature and CO concentration in the protected zone at the other side of the air curtain were shown to be both reduced exponentially significantly with the increase of the discharging velocity of the air curtain. All these indicated that air curtain can be an efficient measure for such application.

Acknowledgements

This work was sponsored by Natural Science Foundation of China (NSFC) under Grant No. 50706050, Anhui Provincial Natural Science Foundation of China under Grant No. 070415224 and China Postdoctoral Science Foundation under Grant No. 20060400203. The partial support from the opening fund of State Key Laboratory of Fire Science under Grant No. HZ2006-KF08 was also appreciated.

References

[1] J. Hietaniemi, R. Kallonen, E. Mikkola, Burning characteristics of selected substances: production of heat, smoke and chemical species, Fire Mater. 23 (4) (1999) 171–185.
[2] J.J. Liu, B. Lan, W.L. Zhang, et al., Experimental study on the smoke components in the underground shopping center fire, Fire Sci. Technol. 1 (1) (2001) 10–12 (in Chinese).
[3] X.Z. Meng, B.F. Yu, F.H. Wang, The study on the air flow and heat transfer of vertical display case, Fluid Mach. 29 (2) (2001) 50–52.
[4] K.B. McGrattan, A. Hamins, D. Stroup, Sprinkler, Smoke & Heat Vent, Draft Curtain Interaction—Large Scale Experiments and Model Development, National Institute of Standards and Technology, Gaithersburg, MD, NISTIR 6196-1, September 1998.
[5] L. Guyonnaud, C. Solliec, Design of air curtains used for area confinement in tunnels, Exp. Fluids 28 (2000) 377–384.
[6] A.M. Foster, M.J. Swain, R. Barrett, P. D'Agaro, S.J. James, Effectiveness and optimum jet velocity for a plane jet air curtain used to restrict cold room infiltration, Int. J. Refrig. 29 (2006) 692–699.
[7] P. Roberson, B.H. Shaw, The linear air curtain as a particulate barrier, J. Environ. Sci. 21 (1978) 32–33.
[8] J. Partyka, Analytical design of an air curtain, Int. J. Model. Simul. 15 (1995) 14–22.
[9] M.A. Szatmary, Isolation chamber air curtain apparatus, Patent WO 98 50134, 1997.
[10] J.P. Rydock, T. Hestad, H. Haugen, J.E. Skaret, An isothermal air curtain for isolation of smoking areas in restaurants, in: H.B. Awbi (Ed.), Air distribution in Rooms (Roomvent 2000), Elsevier, 2000, pp. 664–668.

[11] M. Pavageau, E. Nieto, C. Rey, Odour and VOC confining in large enclosures using air curtains, Water Sci. Technol. 44 (9) (2001) 165–171.
[12] S. Gupta, M. Pavageaua, J.-C. Elicer-Cortes, Cellular confinement of tunnel sections between two air curtains, Build. Environ. 42 (2007) 3352–3365.
[13] H. Sakurai, T. Hayashi, M. Shibata, K. Kanehara, Researches on air shutter for fire defence, Fire Saf. J. 80 (1979) 9–16.
[14] M.S. Altinakar, A. Weatherill, Use of an inclined air curtain for preventing smoke propagation in a tunnel during fire emergency, in: Proceedings of the 4th International Conference on Safety in Road and Rail Tunnels, 2001.
[15] P.A. Friday, F.W. Mowrer, Comparison of FDS Model Predictions with FM/SNL Fire Test Data, National Institute of Standards and Technology, NISTGCR01-810, Gaithersburg, MD, 2001.
[16] K.B. McGrattan, G.P. Forney, Fire Dynamics Simulator (Version 4.07)—User's Guide, National Institute of Standards and Technology, NIST Special Publication 1019, Gaithersburg, MD, 2006.
[17] http://www.nist.gov/fds.
[18] N.L. Ryder, J.A. Sutula, C.F. Schemel, A.J. Hamer, V.V. Brunt, Consequence modeling using the fire dynamics simulator, J. Hazard. Mater. 115 (2004) 149–154.
[19] N.L. Ryder, C.F. Schemel, S.P. Jankiewicz, Near and far field contamination modeling in a large scale enclosure: fire dynamics simulator comparisons with measured observations, J. Hazard. Mater. 130 (2006) 182–186.
[20] L.H. Hu, R. Huo, Y.Z. Li, H.B. Wang, W.K. Chow, Full-scale burning tests on studying smoke temperature and velocity along a corridor, Tunn. Undergr. Space Technol. 20 (3) (2005) 223–229.
[21] L.H. Hu, Y.Z. Li, R. Huo, L. Yi, W.K. Chow, Full-scale experimental studies on mechanical smoke exhaust efficiency in an underground corridor, Build. Environ. 41 (12) (2006) 1622–1630.
[22] L.H. Hu, N.K. Fong, L.Z. Yang, W.K. Chow, Y.Z. Li, R. Huo, Modeling fire-induced smoke spread and carbon monoxide transportation in a long channel: fire dynamics simulator comparisons with measured data, J. Hazard. Mater. 140 (2007) 293–298.